Numerical Analysis of Crack Initiation and Propagation Behaviors in TP-650 Titanium Matrix Composites

W.D. Song[1], J.G. Ning[1], X.N. Mao[2]

[1] State Key Laboratory of Explosion Science and Technology, Beijing Institute of Technology, Beijing 100081, P.R.China
[2] Northwest Institute for Non-ferrous Metal Research, Xi'an, Shanxi 710016, P.R.China

ABSTRACT. *Homogenization theories for periodic microstructures are introduced to investigate the crack initiation and propagation behaviours of the TP-650 titanium matrix composites. By adopting homogenization theories for periodical microstructures, the macroscopic material parameters are identified by solving the microscopic equations. A new fixed point iteration method for multi-particle unit cell's boundary conditions of the microstructures is presented. The real displacement constrained conditions are obtained and applied to the multi-particle unit cell with this method. Finite element (FE) models containing some microstructure characteristics of the TP-650 composite are established and their fracture behaviors of the composites under tensile loading are simulated.*

INTRODUCTION

The development of metal matrix composites (MMCs) has been one of the major innovations in materials engineering. MMCs are widely considered for structural applications where potential weight-savings can be realized by using light-weight matrices strengthened with strong ceramic phases. Titanium carbide (TiC)-reinforced titanium matrix composites are particularly attractive because of combination of the metallic properties of matrices with the ceramic properties of TiC leading to a composite material with higher modulus, strength, wear resistance, and thermal stability [1-3].

One of the interesting characteristics of these composites is being able to retain good mechanical properties at rather high temperatures. Common titanium alloys can generally be used at temperatures up to about $500\,^{0}C$; higher temperatures can only be tolerated by β titanium alloys containing tailored alloying elements. For serving temperature of the titanium alloys, TiC/TiB is added to improve the mechanical properties, because of their high modulus, high thermal stability and similar density to titanium. For this reason, the Ti/ceramic-particles composites are far advantageous over the aluminium-based MMCs, provided that no detrimental reactions occur between the matrix and ceramic at high temperatures [4].

Northwest Institute for Non-Ferrous Metal Research has recently developed a pre-treatment melt process (PTMP) to manufacture TiC particulate-reinforced composites TP-650 [5-7]. Johnson et al. [8] examined the compressive behaviour at room temperature of Ti-6Al-4V/Tic composites and found that the dominant mechanism of the composites was due to carbon in solid solution. Baroza et al.[9] investigated the creep behaviour of the conventional Ti-6Al-4V alloy under constant load tensile tests and reported that the higher resistance of Tic-6Al-4V could be attributed to α/β interfaces acting as obstacles to dislocation motion and to the average grain size.

With fast development of computers, numerical simulations have been gradually accepted by scientists worldwide [10-14]. Preferred over physical experiments, numerical simulations draw more attraction due to their low cost, easy setting of parameters, and high repeatability. Leon and Mishnaevsky [15] performed 3D finite element simulations of the deformation and damage evolution of SiC particle reinforced Al composites for different microstructures and reported that the strain hardening coefficient increases with varying the particle arrangement in the following order: gradient<random< clustered<regular microstructure and the variations of the particle sizes led to strong decrease in the strain hardening rate of the composite. Drabek and Böhm [16] presented a 3D micromechanical finite element method of metal matrix composites to multi-particle and multi-fiber unit cells and discussed the effects of microgeometrical parameters on the mechanical response. Böhm et al. [17] employed a multi-inclusion unit cell models to study the effects of the reinforcements types and shapes and analyzed the predicted microfields in terms of their phase averages and the corresponding standard deviations.

In the current study, homogenization theories for periodic microstructures are introduced to investigate the crack initiation and propagation behaviors of the TP-650 titanium matrix composites. Based on the fixed point iteration method, the boundary conditions for the microstructures are calculated. After identifying the real displacement constrained conditions for multi-particle unit cell model of the microstructures, finite element (FE) models containing important microstructure characteristics of the TP-650 titanium matrix composites are established and the crack initiation and propagation processes of the composites under tensile loading are simulated.

HOMOGENIZATIN THEORY FOR PERIODIC MICROSTRUCUTRES

The mechanical characteristics of materials with periodic microstructures change smoothly with macroscopic scale x, while the mechanical properties generally possess a high oscillation in a close vicinity of x [18-21]. Thus, two scales were taken into account: macroscopic scale x and microscopic scale y. ε is then introduced to indicate the x/y ratios. That is,

$$y = x/\varepsilon \tag{1}$$

Expanding the structure displacement $u^{\varepsilon}(x)$ as an asymptotic series of a small parameter ε

$$u^{\varepsilon}(x) = u^{0}(x,y) + \varepsilon u^{1}(x,y) + \varepsilon^{2} u^{2}(x,y) + \cdots \tag{2}$$

Substitute Eq.2 into a virtual work equation

$$\int_{\Omega^{\varepsilon}} E_{ijkl} \frac{\partial u_k^{\varepsilon}}{\partial x_l} \frac{\partial v_i}{\partial x_j} d\Omega = \int_{\Omega^{\varepsilon}} f_l^{\varepsilon} v_l d\Omega + \int_{\Gamma_t} t_l v_l d\Gamma + \int_{S^{\varepsilon}} p_l^{\varepsilon} v_l dS \tag{3}$$

where $\mathbf{u}^{\varepsilon}$ and $\mathbf{v}$ are the real e virtual displacements, respectively. $\mathbf{f}$ is the body force applied on the open subset Ω with a smooth boundary on Γ comprising Γ_d (where displacements are prescribed) and Γ_t (the traction boundary), $\mathbf{t}$ and $\mathbf{p}$ are the tractions.

Then, we have：

$$\int_{\Omega^{\varepsilon}} E_{ijkl}^{H} \frac{\partial u_{0k}}{\partial x_l} \frac{\partial v_{0l}}{\partial x_j} d\Omega = \int_{\Omega^{\varepsilon}} f_l^{\varepsilon} v_{0l} d\Omega + \int_{\Gamma_t} t_l v_{0l} d\Gamma + \int_{S^{\varepsilon}} p_l^{\varepsilon} v_{0l} dS \tag{4}$$

where E_{ijkl}^{H} is the effective elastic tensor that is defined by Eq.5

$$E_{ijkl}^{H} = \frac{1}{|Y|} \int_{Y} E_{ijkl} - E_{ijmn} \frac{\partial \boldsymbol{\chi}_m^{kl}}{\partial y_n} dY \tag{5}$$

where $\boldsymbol{\chi}_m^{kl}$ is the periodic solution of the following homogenization equation:

$$\int_{Y} E_{ijkl} \frac{\partial v_i}{\partial y_i} dY = \int_{Y} E_{ijmn} \frac{\partial \boldsymbol{\chi}_m^{kl}}{\partial y_n} \frac{\partial v_i}{\partial y_j} dY = 0, \forall v \in V_Y \tag{6}$$

where Y is the period. Eqs.5 and 6 present the macroscopic and microscopic homogenization problems, respectively. By solving the microscopic ones, the macroscopic material parameters can be calculated, whereas the microscopic boundary conditions can be identified from the macroscopic ones.

FIXED POINT ITERATION AND FINITE ELEMENT ANALYSIS

The solution of the effective mechanical parameters of composites with periodic microstructures can be used to solve the nonlinear functional equation

$\Phi\left(\xi_{\mathrm{m}}, \xi_{\mathrm{p}}, f, u, \xi\right)=0$. ξ_{m} and ξ_{p} are the mechanical parameters of the matrix and reinforcement, respectively. ξ is the effective mechanical parameter of the composite. The solution for $\Phi\left(\xi_{\mathrm{m}}, \xi_{\mathrm{p}}, f, u, \xi\right)=0$ is known to exit and has a single value. According to the Banach fixed point theorem[22], the fixed point ξ can be calculated by repeated iteration, only if an initial value ξ_0 and a compression mapping are found on the basis of $\Phi\left(\xi_{\mathrm{m}}, \xi_{\mathrm{p}}, f, u, \xi\right)=0$.

The microstructure of composites is assumed as a periodic and repeating array of a heterogeneous unit cell. In Fig.1, a macroscopic homogeneous model was established by assuming $\xi_0=\xi_{\mathrm{m}}$. The freedom of the left end of the model is constrained, and to the right end, uniform tensile loading is applied. An area having the same size of a unit cell is subsequently chosen. The displacement values of all the nodes of the boundary in the area are identified from the calculation results. In Fig.2, a multi-particle unit cell model is established by applying the displacement values on the corresponding nodes. The displacement boundary conditions for the other nodes are identified by the linear interpolation of the known nodes. The next step is to solve the boundary values. The effective mechanical parameter ξ_1 can be calculated on the basis of the $\sigma_{\mathrm{e}}-\varepsilon_{\mathrm{e}}$ curve plotted by the numerical results. Then, another macroscopic homogeneous model is established by using ξ_1 , and the rest may be deduced by analogy until $\xi_{\mathrm{n+1}}-\xi_n \leq \varepsilon$ (ε is a negligible value). ξ_n is the solution when $\Phi(\xi_1, \xi_2, f, u, \xi)=0$ and is also the effective mechanical parameter of the composites. The boundary condition Γ_n presents the real boundariy movement of the unit cell in the composite under sinple tension.

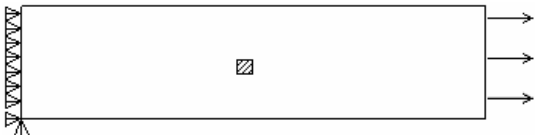

Fig.1 Schematic of the homogenous material model

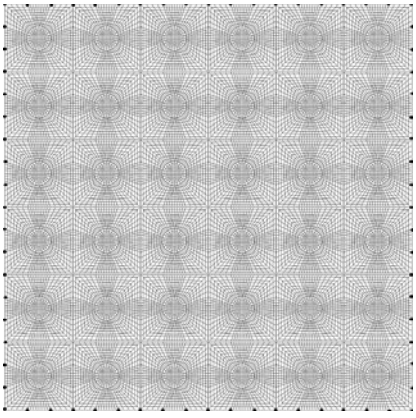

Fig.2 A finite element model of a multi-particle unit cell

Material models and material parameters

LS-DYNA, an explicit finite element program developed by Livermore Software Technology Corporation is adopted in this section to investigate the fracture behavior of TP-650 titanium matrix composites. A plastic kinematic material model and an elastic model are used to simulate the matrix and the reinforcement, respectively. Plane162, a 2D and 4 nodes solid element provided by LS-Dyna, is used in present numerical simulations.Table.1 lists the mechanical parameters of the particle and matrix.

Table.1 Mechanical parameters of TiC and titanium alloy matrix

Material	TiC particle	T650 matrix
ρ / g/cm^3	4.43	4.51
E /GPa	460	108
v	0.188	0.35
σ_s/MPa		1095
E_t /GPa		6e-2
C/s^{-1}		1832.6
P		2.3

Micro-crack initiation and propagation of theTP-650 composites

A multi-particle unit cell model of TP-650 composites is established. The model contains 36 particles with the size of 5μm and the volume fraction of the composite is 3%. In order to simply numerical simulations, the interfaces between the TiCp and the matrix are considered to be perfect. Then, the displacement values obtained from the iteration process are applied on the finite element model with 36 particles. It can be seen from Fig.3 that there is no damage in the model at t = 3μs and the maximum stress occurred at the bottom of the model.

Fig.4 shows the stress-time history curve. Seen from this figure, it can be observed that:

(1) 0～8μs，the stress increases rapidly with a high rate of slope and the maximum value is about 1.1GPa.

(2) 9～14μs，the stress increase slowly. The reason is that some micro-cracks occured in this stage, while these miro-cracks exert no obvious influence on the bearing ability .

(3) 15～39μs，the stress begin to reduce. In this stage, the microcracks propagte quickly and connect with each other causing the rapid reduction of the stress peak vlues.

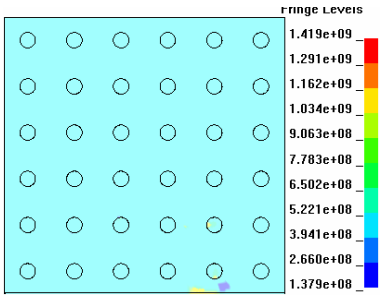

Figure. 3 Stress distribution in multi-particle unit cell model at $t = 3\mu s$

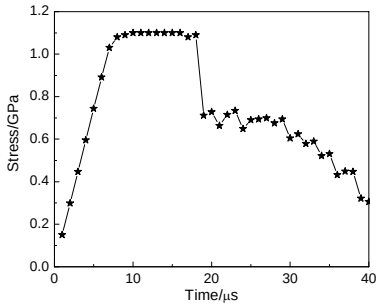

Figure.4 Stress-time history curve

Fig.5 demonstrates the crack initaion and propagation behavior of the TP-650 composites in a multi-particle unit cell model for the load case of macroscopic uniaxial tensile loading in the horizontal direction. First, a crack can be clearly found at the right corner near the bottom of the model and then another crack initiates and propagates throughout the matrix, while the first one grows slowly. It is found that the crack goes around a particle at the right corner of the top and spreads through the matrix. As the loading time increases, a few other cracks occur in the left side of the unit cell, some of them being mutually connected, which results in the failure of the material.

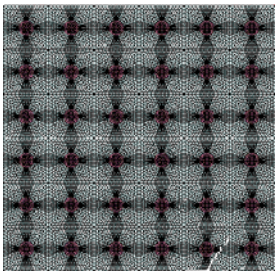

$t = 17\mu s$

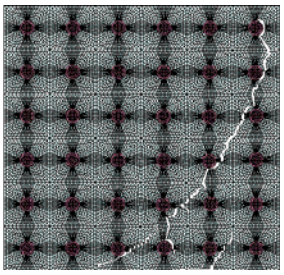

$t = 22\mu s$

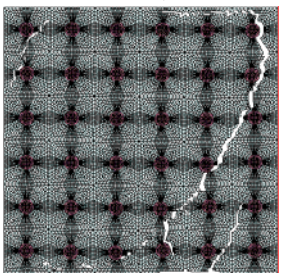

$t = 33\mu s$

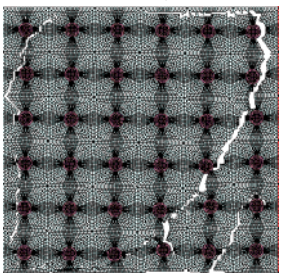

$t = 38\mu s$

Figure.5 Predicted progress of a crack in a multi-particle unit cell of TP-650

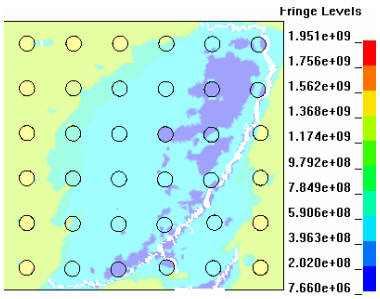

Figure. 6 Stress distribution in multi-particle unit cell model at $t = 29\mu s$

Fig.6 shows the stress field of the model at $t = 29\mu s$. Seen from this figure, it can be observed that the stress in the vicinity of micro-crack areas begin to unload and possess a lower value, while the stress in the areas with no microcracks presnents a higher value. With the crack propagation, the stress field will be redistributed.

From the above numerical simulations, the crack initaion and propagation behavior of TP-650 titanium matrix composites are complicated because of the interactions among the particles, especially the stress redistribution caused by the crack propagation.

CONCLUSIONS

Homogenization theories are introduced to study the relationship of microstructure parameters with the mechanical response of TP-650 titanium matrix composites. A new fixed point iteration method is presented to provide boundary conditions for the mcirostructures. Finite element (FE) models of a multi-particle unit cell are established. A series of cases are performed to explore the fracture characteristics of the composites under tensile loading are simulated. The particle is found to have certain influences over the micro-crack propagation.

ACNOWLEDGEMENTS

This study is supported by the National Nature Science Foundation of China (10625208, 10602008) and Northwest Institute for Non-Ferrous Metal Research.

REFERENCES

1. Lv W.J., Zhang D. (2005) *Fabrication, microstructure and mechanical properties of in situ synthesized titanium matrix composites.* Higher Education Press, Beijing.

2. Liu G., Zhu D., Shang J-K. (1993) *Scripta Metall Mater.* 28, 729-32.
3. Feng C.R., Michel D.J., Crowe C.R. (1989) *Scripta. Metall.* 23, 241-46.
4. Badini C., Ubertalli G., Puppo D. (2000) *J. Mater. Sci.* 35, 3903-12.
5. Mao X.N., Zhou L., Zeng Q.P, et al. (2000) *Rare Metal Mater. Eng.* 29, 218-20.
6. Mao X.N., Zhou L., Zhou Y.G., et al. (2004) *Rare Metal Mater. Eng.* 33, 620-23.
7. Zhang Y.J., Zeng Q.P., Mao X.N., et al. (1999) *Rare Metal Mater. Eng.* 28, 265-68.
8. Wagoner Johnson A.J., Kumar K.S., Btiant C.L. (2003) *Metall. Mater. Trans. A* 34A:1869-1877.
9. Barboza M.J.R., Perez E.A.C., Medeiros M.M., et al. (2006) *Mater. Sci. Eng. A* 428:319-326.
10. Bush M.B. (1992) *Mater. Sci. Eng.* A154, 139–148.
11. Loretto M.H., Konitzer D.G. (1990) *Metall Mater Trans.* 21, 1579-87.
12. Song W.D., Ning J.G., Wang J. (2008) *Int. J. Impact Eng*. 35:1022-1034.
13. Zhang R., Lu. X.N. (1995) *Acta Materiae Compositae Sinica*. 12(4), 91-93.
14. Song W.D., Ning J.G., Liu H.Y. (2008) *Int. J. Mod. Phys. B* 22(31/32): 5453-5458.
15. Leon L., Mishnaevsky Jr. (2004) *Acta Mater.* 52:4177-4188.
16. Drabek T., Böhm H.J. (2006) *Comput. Mater. Sci.* 37:29-36.
17. Böhm H.J., Eckschlager A., Han W. (2002) *Comput. Mater. Sci.* 25:42-53.
18. Hassani B., Hinton E. (1998) *Comput. Struct.* 69,707-717.
19. Hassani B., Hinton E. (1998) *Comput. Struct.* 69,719-738.
20. Hassani B., Hinton E. (1998) *Comput. Struct.* 69,739-756.
21. Kreyszing E. (1987) *Introductory Functional Analysis with Applications*, Beihang University Press, Beijing.